DOI: 10.1002/ejic.200700128

Electronic Structures and Spectroscopic Properties of $[Pt(CNMe)_2(CN)_2]_n$ (n = 1–4): A Theoretical Exploration of Promising Phosphorescent Materials

Xin Zhou,[a] Hong-Xing Zhang,*[a] Qing-Jiang Pan,[b] Ming-Xia Li,[a,b] Yue Wang,[c] and Chi-Ming Che[d]

Keywords: Ab initio calculations / DFT calculations / Luminescence / Excited states / Platinum(II) oligomer

The structures of $[Pt(CNMe)_2(CN)_2]_n$ (n = 1–4) in the ground states (S_0) and lowest-energy triplet excited states (T_1) were calculated by using the second-order Møller–Plesset perturbation (MP2) and density functional theory (DFT) methods, respectively. The MP2 results show that the formation of the dimer causes a significant red shift in emission energy, and the frequency calculations reveal that a weak metal–metal interaction exists in the S_0 state, which is greatly enhanced in the $^3[d_\sigma \cdot p_\sigma]$ excited state. The aggregation of $[Pt(CNMe)_2(CN)_2]_n$ (n = 1–4) was explored by using the slate-type VWN functional in the DFT method. The $^3B_u \rightarrow {}^1A_g$ transition in the dimer at 509 nm corresponds to the experimental higher-energy emission at 530 nm in CH_3CN solution, while the $^3A' \rightarrow {}^1A'$ transitions in the trimer and tetramer at 557 and 650 nm, respectively, are responsible for the low-energy emission at 584 nm observed experimentally. The analyses of the Wiberg bond indices for the Pt–Pt bond indicate that the dimer may be the most stable form in solution and that the oligomer species (n = 3 and 4) can be treated as a special dimer in which the excess z electron ligand is bonded to the Pt atoms of the central dimer.

Introduction

In the past three decades, there has been a continuous interest in luminescent platinum(II) complexes. The distinctive molecular and electronic structures that occur in d^8 platinum(II) systems give rise to some unusual and potentially useful excited-state properties, in particular, those containing weak d^8–d^8 interaction in the range of 2.7–3.5 Å.[1] Generally, Pt^{II}–Pt^{II} contacts exist not only in the solid state but also in solution. Unusual colors and strong emissions, as well as highly anisotropic properties, are often the result of such stacking interactions. Platinum(II) complexes having a weak Pt–Pt interaction are classified into two types: (a) dimers with bridging ligands connecting two platinum(II) atoms[2] and (b) one-dimensional (1D) linear-chain platinum(II) oligomers with a zigzag Pt–Pt–Pt chain stacked equidistantly.[3]

Platinum(II) dimers have been extensively investigated in the last century. For example, $[Pt_2(pop)_4]^{4-}$ (pop^{2-} = $P_2O_5H_2^{2-}$) with rich photophysical and photochemical properties greatly motivated the study of binuclear d^8 complexes.[2a,2b,4–11] The light-induced $^3A_{2u}$ excited state of $[Pt_2(pop)_4]^{4-}$ is highly reactive. It reacts with a wide range of quenchers by mechanisms that involve the platinum complex as an oxidant, reductant, or atom-transfer reagent. Coppens[12a] and Rillema[12b] have investigated $[Pt_2(pop)_4]^{4-}$ by DFT, and the featured absorptions and emissions were attributed to the metal-localized $\sigma^*(d) \rightarrow \sigma(p)$ transition. Another case is the well-studied *trans*-$[Pt_2(CN)_4(PR_2CH_2PR_2)_2]$ (R = Me and cyclohexyl) and *trans*-$[Pt_2(CN)_4(PPh_2CH_2PPh_2)_2]$ complexes.[2c–2f] These platinum(II) dimers exhibit an intense emission both in the solid state and in solution at room temperature in the visible region, which has been assigned to a $\sigma(p) \rightarrow \sigma^*(d)$ (metal-centered, MC) transition. Recently, a great interest in 1D platinum(II) linear structures has developed because they are expected to play a critical role in the fabrication of nanodevices with novel electrical, magnetic, and optical properties. The most-investigated 1D platinum(II) complex with a linear-chain structure is platinum(II) polypyridine.[3] Compounds with polypyridyl ligands show intense luminescence and typically exhibit $\pi^*(L) \rightarrow d_{\sigma^*}$ (Pt) emission from a metal-metal-to-ligand-charge-transfer (MMLCT) excited state. Furthermore, the nature and lifetime of the excited

[a] State Key Laboratory of Theoretical and Computational Chemistry, Institute of Theoretical Chemistry, Jilin University, Changchun 130023, China
Fax: +86-431-8945942
E-mail:zhanghx@jlu.edu.cn
[b] School of Chemistry and Materials Science, Heilongjiang University, Haerbin 150080, China
[c] Key Laboratory for Supramolecular Structure and Materials of the Ministry of Education College of Chemistry, Jilin University Changchun 130012, China
[d] Department of Chemistry and HKU-CAS Joint Laboratory on New Materials, University of Hong Kong, Pokfulam Road, Hong Kong SAR, China

Supporting information for this article is available on the WWW under http://www.eurjic.org or from the author.

state of these complexes can be changed greatly through modifying the ligands.

In our previous works, Wang and Che et al. found that $[Pt(CNtBu)_2(CN)_2]$[13] can form 1D luminescent nanowires through weak Pt–Pt interactions, which are rare in the reported self-assembly 1D architectures. As suggested, the metal-localized $5d_{\sigma^*} \rightarrow 6p_{\sigma}$ transition of $[Pt(CNtBu)_2(CN)_2]_2$ can lead to the effective construction of 1D functional nanomaterials and intense green emission; the oligomerization of the monomers does impact on the luminescence behavior and the electronic structures. In fact, similar neutral platinum(II) complexes with the general formulas $[Pt(CNR)_4][Pt(CN)_4]$ and $[Pt(CNR)_2(CN)_2]_2$ (R = alkyl and aryl) have been extensively studied by Mann and coworkers.[14] However, their investigation was limited to their application towards chemical sensors and their vapochromic behavior, and there was little discussion on their luminescence properties and the effect of oligomerization on the luminescence and the electronic structures. Furthermore, to the best of our knowledge, the luminescent properties for oligomerized $[Pt(CNtBu)_2(CN)_2]_n$ have not been theoretically investigated for the platinum(II) complexes.

In this paper, we have examined the ground- and excited-state properties of $[Pt(CNMe)_2(CN)_2]_n$ (n = 1–4) by using ab initio and DFT calculations. We aimed at elucidating three points: (1) the ground- and excited-state geometrical and electronic structures of $[Pt(CNMe)_2(CN)_2]_n$ (n = 1–4), (2) the relationship between the weak Pt^{II}–Pt^{II} interaction and the electronic structure as well as the luminescence properties, (3) whether the oligomerization of the platinum(II) chain will strengthen the weak inter- and/or intra-interaction in solution and lower the emission energies. Here we present the study of the electronic structures, geometrical structures, and spectroscopic properties.

Computational Details

$[Pt(CNMe)_2(CN)_2]$ was used as the computational model to represent the real complex $[Pt(CNtBu)_2(CN)_2]$. This strategy was employed in our previous work to save computational cost, and it proved to be suitable for reproducing the experimental results.[15]

The electronic structures and emission spectra of monomer $[Pt(CNMe)_2(CN)_2]$ (**1**) and dimer $[Pt(CNMe)_2(CN)_2]_2$ (**2**) were carried out with the Gaussian 03 program package (G03).[16] Full optimizations on the ground state (S_0) and lowest-energy triplet excited state (T_1) were performed at the second-order Møller–Plesset perturbation (MP2) and UMP2 levels of theory, respectively.[17] On the basis of the optimized T_1 geometries of the complexes, we employed the time-dependent density functional theory (TDDFT)[18] method at the PBE0 functional level[19] to predict the emission spectra. By considering the differences in the emission spectra in gas and solution, the solvent effect of acetonitrile was taken into account by using the polarizable continuum model (PCM).[20] The above calculations were performed by using the LanL2DZ basis sets with effective core potentials (ECPs) for the Pt atom proposed by Hay and Wadt.[21] To describe the Pt–Pt interaction and the molecular properties precisely, one additional function was implemented for the Pt atom (α_f = 0.14).[22]

One of the objectives of this paper is to discuss whether the formation of oligomers can affect the electronic structure and emission energy of $[Pt(CNMe)_2(CN)_2]_n$. However, to achieve these goals with ab initio calculations will require very long computational resources, because we are dealing with large oligomers containing rather heavy atoms, the modeling of which requires an extremely large number of basis functions. Therefore, in order to pursue these goals, we performed DFT calculations with relativistic effects by using the Amsterdam Density Functional (ADF2005.01) program.[23] As concluded by Pyykkö,[24] the weakly- or non-overlapping systems are not reasonably calculated by the DFT method, because the dispersion interaction of R^{-6} is not explicitly included in the present DFT method. Nevertheless, in some recent papers, it was reported that the experimental results of weak metal–metal bonding can be reproduced by a simple local density functional (such as SVWN or Xα), rather than the gradient corrected density functionals (DFs) [B3LYP, BLYP, BP86, and PBE0].[25] Although the intrinsic reason is not yet clear, the application of the DFT approach to study large oligomers seems to be feasible. Similar $[AuCN_2^-]_n$ oligomers have been studied with Extended Hückel calculations, and the corresponding results were satisfactory.[26]

In the ADF calculations, the geometrical structures of $[Pt(CNMe)_2(CN)_2]_n$ (n = 1–4) in the S_0 and T_1 states were optimized by spin-restricted and spin-unrestricted Vosko–Wilk–Nusair (VWN) calculations, respectively.[27] The valence atomic orbitals of the platinum, nitrogen, carbon, and hydrogen atoms were described by the TZP basis sets. The cores (1s2s2p3s3p4s4p for Pt and 1s for C, N and O) were kept frozen. Relativistic effects were included by means of the Zero Order Regular Approximation (ZORA).[28] TDDFT (PBE0) calculations were performed on the equilibrium excited-state geometries of $[Pt(CNMe)_2(CN)_2]_n$. The conductor-like screening model (COSMO)[29] was used to simulate the solvent effects, as implemented in the ADF code. In order to describe the asymptotic behavior well, a combination of the local VWN and the Becke–Perdew (BP86)[30] gradient correction term was employed.

Results and Discussion

The Monomer and Dimer in the S_0 State

In this work, C_{2v} symmetry is assigned to monomer **1**, with the two mutually *cis* CN ligands. For dimer **2**, the initial C_1 symmetry is adopted with a torsion angle C1–Pt1–Pt2–C3 of 55°, as indicated in the X-ray results. The torsion angle is subjected to geometry optimization and decreases by ca. 0.2° for the dimer, the framework of which is close to C_{2h} symmetry. Such a big difference in the torsion angle results from the replacement of *tert*-butyl groups used experimentally by methyl groups used in the calculation. As

a result, the steric repulsion between the bulky *tert*-butyl groups is eliminated, and the torsion angle is greatly reduced. Therefore, the C_{2h} symmetry for the dimer is adopted throughout this paper. The optimized S_0 structures of the platinum(II) monomer and dimer, with the coordination axis, are depicted in Figure 1, and the corresponding important parameters are listed in Table 1. As shown in Table 1, the geometrical parameters for the monomer and dimer are very close and agree well with most of the experimental values for $[Pt(CN)_4^{2-}]$ ions and for double salts such as $[Pt(CNR)_4(CN)_4]$ (R = toluene),[14] which indicates that the eclipsed structures do not have an impact on the geometrical structure of the monomer. The Pt–C1 and C1≡N1 bonds are ca. 0.017 and 0.023 Å longer than the Pt–C2 and C2≡N2 bonds. The small increase in length results from the different electronic structures of the *iso*cyanide and cyanide ligands as discussed in most textbooks. The C1≡N1 and C2≡N2 bonds are slightly long, but fall in the range of C≡N distances generally measured experimentally for these types of complexes. The deviations are thought to arise because the experimental values are measured with rather large uncertainties and because smaller basis sets are applied to the C and N atoms. To test the dependence of the Pt–C and C≡N bond lengths on the basis sets, we optimized **1** at the MP2 level with different basis sets (Table S1). The results suggest that with the increase in the size of the basis sets (BS I–VII), the lengths of the Pt–C and C≡N bonds decrease greatly and are much closer to the experimental values. Because the Pt–Pt bond is obviously shortened, a definite hydrogen bond between the N (CN) and H (Me) atoms is formed and the N1–H1 bond length is 2.468 Å, which falls within the normal range of hydrogen bond lengths. Further, the stacking of $[Pt(CNMe)_2(CN)_2]_2$ may be partially stabilized by hydrogen bonds in the solid state and in solution. In addition, the formation of the hydrogen bond gives rise to a tilted angle of 9.6° for the Pt–Pt vector relative to the *z* axis, which is in accordance with that observed experimentally.

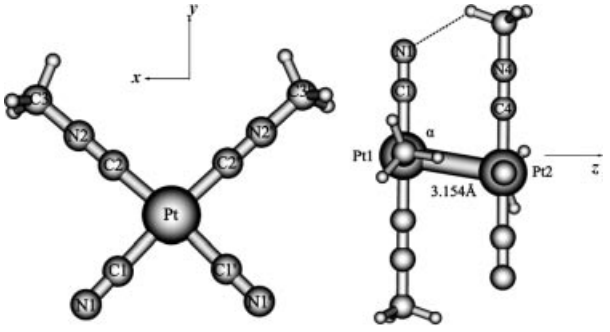

Figure 1. Optimized S_0 structures for **1**–**2** determined by MP2 methods.

The most important Pt–Pt bond length was calculated to be 3.154 Å, which falls in the usual range for most platinum(II) dimers (2.7–3.5 Å) and is comparable to those calculated previously for the $[Pt_2(pop)_4]^{4-}$ and $[Pt_2(pop)_4]^{4-}$ ions[15c] and for the neutral molecule $[Pt_2(CN)_4(PH_2CH_2PH_2)_2]$.[31] The slightly shorter Pt–Pt distance than the van der Waals contact of 3.2 Å indicates the presence of a possible weak bonding interaction between the two Pt^{II} centers in **2**. It should also be noted that the calculated Pt–Pt bond length is ca. 0.2 Å shorter than that determined by X-ray diffraction. This is because excess electron correlation effects are included in the MP2 calculation (which considerably shortens the Pt–Pt bond length) and because methyl groups are used in the calculation. To evaluate the interaction strength between the two monomers, the interaction energy is obtained by taking into account the counterpoise (CP) correction; these results are summarized in Table 1. The calculated interaction energy after CP correction is ca. 35 kJ/mol, comparable to that of hydrogen bonds. The interaction energy should result from three contributions. In addition to the contribution from the metallophilic interaction between Pt–Pt and from the hydrogen bond of N1–H1, the attraction between the π-electron clouds of CN^- and *iso*-CN^- also partially contributes to the interaction energy. To further understand the Pt–Pt bonding nature, the frequency calculation was preformed on the dimer (Table 1). Table 1 shows that the stretching vibration of Pt–Pt is 87 cm^{-1} and the force constant is 0.309 mDyne/A. The two values agree well with those in systems in which there are weak Au^I–Au^I interactions,[26] and suggest the presence of Pt–Pt bonding. The MO diagram of **2**, represented in Figure 2, is used to elucidate the formation of the Pt–Pt bond. The fully occupied $5d_{z^2}$ atomic orbitals of adjacent platinum centers split to give d_σ bonding and d_{σ^*} antibonding molecular orbitals, as has been reported in other papers.[32] Similarly, the unoccupied $6p_z$ atomic orbitals split to give p_σ and p_{σ^*} molecular orbitals. There exist two kinds of

Table 1. Optimized S_0 and T_1 geometrical parameters for **1**–**2** determined by MP2 calculations.

	Bond length [Å]						Bond angle [°]				Frequency		ΔE
	Pt–Pt	Pt–C1	Pt–C2	C1≡N1	C2≡N2	N1–H1	C1–Pt–C2	C2–Pt–C2′	C1–Pt–C2′	α	ν_{Pt-Pt} [cm^{-1}]	k(Pt–Pt) [mDyne/A]	[kJ mol^{-1}][a]
monomer													
$^1A_1$	–	2.014	1.995	1.219	1.198	–	87.6	95.5	176.9	–	–	–	–
$^3B_2$	–	2.011	2.036	1.156	1.191	–	91.3	90.0	178.7	–	–	–	–
dimer													
^1A_g	3.154	2.013	1.998	1.220	1.195	2.468	89.1	98.0	178.4	105.4	87.7	0.3090	32
(Exp.)	(3.354)					(2.66)							
^3B_u	2.830	2.022	2.014	1.167	1.186	2.696	91.0	89.9	173.5	101.1	115.6	0.4522	176

[a] Interaction energy between two monomers after counterpoise correction.

bonding interactions between two platinum(II) atoms: the first interaction is a four-electron repulsion between the d_{z^2} orbitals that prevents the two platinum(II) atoms from approaching one another, and the second interaction is a bonding donor–acceptor interaction between the d_{z^2} and p_z orbitals. The combination of the two interactions can account for the weak Pt–Pt bonding.

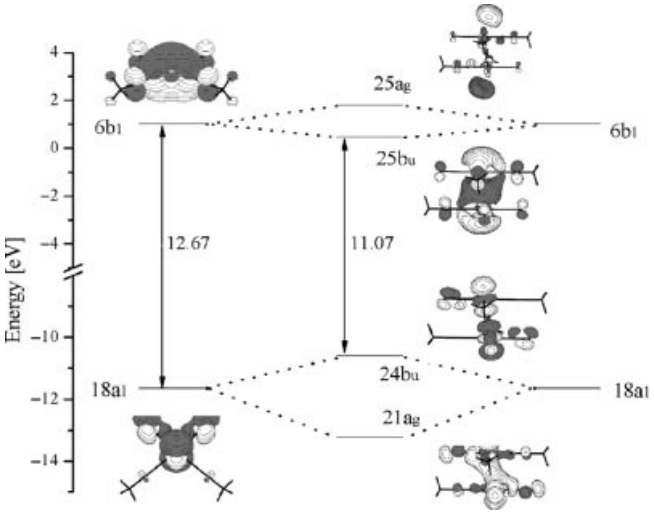

Figure 2. Energy level of **2**.

Monomer and Dimer in the T_1 State and Lowest-Energy Emission Spectra

The structures of **1** and **2** in the T_1 states were determined by the UMP2 method. Optimizations on **1** and **2** predict that their T_1 states have $^3B_2$ and ^3B_u symmetry, respectively. Selected structural parameters are listed in Table 1. The T_1 geometries of the monomer and dimer are found to differ from those in the S_0 state. Both the Pt–C1 and Pt–C2 bonds are elongated slightly in the T_1 state. The formation of Pt–Pt single bond in the T_1 state weakens the Pt–C covalent bonds and Pt←C dative bonds, which can account for the elongation of the Pt–C bond. The C1–N1 and C2–N2 bonds are shorter in the S_0 state than in the T_1 state, in particular, the C1–N1 bond length is reduced by roughly 5.0%. For the dimer, the Pt–Pt distance decreases by ca. 0.324 Å on going from the S_0 state to the T_1 state, while the N1–H1 distance increases by ca. 0.23 Å. The opposite trend for the Pt–Pt and N1–H1 bond lengths implies that the hydrogen bonding of N1–H1 only plays a secondary role in the stabilization of the dimer. Upon excitation, the coordination geometry of the platinum(II) atom is much closer to the regular square-planar structure, as indicated by the C1–Pt–C2 and C2–Pt–C2′ bond angles of ca. 90°. The tilted angle α for **2** decreases by ca. 4°, which suggests that the complex has a straighter chain in the T_1 state. We performed the frequency calculation for the optimized geometry of T_1 at the UMP2 level for **2** in order to further characterize the Pt–Pt bonding in the excited state (Table 1). Table 1 shows that Pt–Pt stretching frequency undergoes a moderate increase from ca. 87.7 to 116 cm^{-1}, and the force constant increases by ca. 0.15, which is consistent with a single electron that is promoted from the d_{σ^*} antibonding to p_σ bonding orbital and with the formation of Pt–Pt single bond in the excited state. In addition, the calculated overlap population between the two Pt atoms is 0.0278 and 0.0169 for the ^3B_u excited state and ^1A_g ground state, respectively. From such calculated frequencies and overlap populations between the two Pt atoms, it can easily be seen that the Pt–Pt interaction in the former is stronger. This suggests that there may be some electron transfer to the 6p bonding orbitals of the Pt atoms. More evidence for the enhancement of the Pt–Pt bonding is the increased interaction energy between the two monomers. UMP2 calculations show that the interaction energy is ca. 176 kJ mol^{-1}, which is of the same order of magnitude as that for the covalent bonding energy. All of the above results illustrate the obvious contraction of Pt–Pt bond that results from the formation of single bond between the two platinum(II) atoms. The conclusion is in agreement with other weakly interacting systems involving heavy transition metals such as Au^I and Pt^{II} etc.[12,26,33]

According to the Franck–Condon vertical transition principle, the emission properties of **1** and **2** were calculated on the basis of their corresponding T_1 geometries. Complexes **1** and **2** give rise to the lowest-energy phosphorescent emissions at 301 and 512 nm (Table 2), which mainly originate from the excited states with the transitions $^3B_1 \rightarrow {}^1A_1$ and $^3B_u \rightarrow {}^1A_g$, respectively. Table 3 gives the partial MO compositions for the two complexes in the phosphorescence, the results from which can be used to further shed light on the emission nature. With respect to the $^3B_1 \rightarrow {}^1A_1$ transition of **1**, the $19a_1 \rightarrow 6b_1$ configuration has the largest CI coefficient of ca. 0.72. As shown in Table 3, the MO $19a_1$ (HOMO) results largely from the contributions of the Pt d_{z^2} orbital (83.6%), whereas the MO $6b_1$ (LUMO) is localized on the Pt p_z and *iso*-CN^- π* orbital. Therefore, the calculation shows that the $^3B_1$ excited state of **1** can give rise to the $p_z/\pi^*(iso\text{-}CN^-) \rightarrow d_{z^2}$ phosphorescent emission. With regard to the $^3B_u \rightarrow {}^1A_g$ transition of **2**, the configuration of $24b_u \rightarrow 25a_g$ corresponds to the largest CI coefficient of ca. 0.72. Analyses of the wavefunctions of the ^3B_u excited state of **2** indicate that the $24b_u$ orbital (HOMO) is a σ* antibonding orbital that results from the Pt $5d_{z^2}$ atomic orbital, and the $25a_g$ orbital (LUMO) has bonding charac-

Table 2. Emissions of **1** and **2** in CH_3CN solution determined by TD-DFT (PBE0) calculations.

	Transition	Configuration (CI coefficients)	*E* [eV] (λ [nm]) Calcd.	Exp.	Assignment
monomer	$^3B_1 \rightarrow {}^1A_1$	$19a_1 \rightarrow 6b_1$(0.72)	4.12(301)	–	$d_{z^2} \rightarrow p_z$
dimer	$^3B_u \rightarrow {}^1A_g$	$24b_u \rightarrow 25a_g$(0.72)	2.42 (512)	2.29 (542)	$5d_{\sigma^*} \rightarrow 6p_\sigma$

ter that arises mainly from the Pt $6p_z$ atomic orbital. Thus, we assign the 512 nm phosphorescence as a $\sigma[p_z(Pt_2)]\rightarrow\sigma^*[d_{z^2}(Pt_2)]$ transition from the triplet to the singlet S_0 state, which is comparable to the 542 nm phosphorescence observed experimentally.

Table 3. HOMO and LUMO compositions (%) of the phosphorescent emissions for **1** and **2** in CH_3CN solution.

Orbital	*E* [eV]	Composition [%] Pt s	Pt p	Pt d	CN	*Iso*-CN	CH_3
monomer							
$6b_1$[a]	–2.0033	–	$24.1p_z$	2.3	11.4	54.9	0.3
$19a_1$[b]	–7.5441	11.0	–	$83.6d_{z^2}$	3.5	1.9	–
dimer							
$25a_g$[a]	–3.2651	1.2	$27.2p_z$	4.2	14.6	46.4	0.6
$24b_u$[b]	–5.8108	5.4	$3.0p_z$	$76.2d_{z^2}$	8.4	6.0	0.4

[a] LUMO. [b] HOMO.

The $[Pt(CNMe)_2(CN)_2]_n$ (n = 1–4) in the S_0 and T_1 States

In previous experimental work,[13] it was found that the emission of $[Pt(CNtBu)_2(CN)_2]$ at 542 nm can be resolved into two bands at 530 and 584 nm, which suggests that two different emissions originate from $[Pt(CNtBu)_2(CN)_2]_n$ oligomers with different values of n in CH_3CN solution. Similar split bands have also been observed in most platinum(II) dimers that exhibit rich excited states such as ^{1,3}MLCT, ^{1,3}ILCT, and $^3\pi$–π transition. However, the various excited states are mostly dominated by the different ligands not by the stacking of the oligomers. Thus, our interest is in whether oligomerization might occur in CH_3CN solution and in the consequent change in geometry and luminescence behavior. In fact, the photophysics of $[Pt(CN)_4^{2-}]_n$[34] with n = 1–5 has been experimentally investigated by Schindler and co-workers in detail; different absorption bands were attributed to the $^1[5d_{\sigma^*},6p_\sigma]$ and $^3[5d_{\sigma^*},6p_\sigma]$ excited states for different values of n. Nevertheless, to the best of our knowledge, there is no theoretical study on the electronic structure and luminescence for similar platinum(II) compounds that are affected by the degree of oligomerization.

The DF approach was employed to obtain the geometrical and electronic structures for $[Pt(CNMe)_2(CN)_2]_n$ (n = 1–4, **1**–**4**). Because the choice of functional is very important for the reproduction of the weak interaction for multiplatinum(II) complexes, the optimization of dimer $[Pt(CNMe)_2(CN)_2]_2$ was carried out with several different versions of the exchange-correlation DF (BP86, PBE0, BLYP, and VWN) to test which DF is better suited to the $[Pt(CNMe)_2(CN)_2]_n$ species. Table S2 presents the partial geometrical parameters of the $[Pt(CNMe)_2(CN)_2]_2$ species. The results show that, analogous to those found in Au^I clusters,[25] the most important Pt–Pt distance was reproduced well by the VWN DF (3.257 Å) but not by the DF involving the gradient-corrected (GGA) exchange potential (BLYP: 3.631 Å, BP86: 3.505 Å, PBE0: 3.498 Å). Therefore, all the $[Pt(CNMe)_2(CN)_2]_n$ (n = 1–4) species were investigated by using the local VWN DF. The Pt–Pt parameters for **1**–**4** are shown in Table 4, and the complete data are tabulated in Table S3. As depicted in Table 4, the Pt–Pt bond lengths are sensitive to n, and all compounds show stronger Pt–Pt bonding in the T_1 state than in the S_0 state, which is reflected by the shorter Pt–Pt equilibrium distances. The Pt–C bond length of **1** and **2** (Table S3) is in agreement with those obtained by the MP2 calculations, but the C≡N bond length is ca. 0.06 Å shorter than those obtained by the MP2 calculations with small basis sets (BS I) and compares to those from calculations with the largest basis set (BS VII). This result is not surprising because the MP2 method is known to be unreliable in the prediction of triple bond lengths.[31]

Table 4. Optimized S_0 and T_1 geometrical parameters in **2**–**4** determined by DFT (VWN) calculations.

		Pt1–Pt2 [Å]	Pt2–Pt3 [Å]	Pt1–Pt2–Pt3 [°]	α [°]
dimer	^1A_g	3.257	–	–	104.8
	^3B_u	2.819	–	–	99.6
trimer	$^1A'$	3.225	3.260	130.8	107.9
	$^3A'$	2.954	3.000	142.0	105.7
tetramer	$^1A'$	3.282	3.187	135.3	106.1
	$^3A'$	3.091	2.936	156.9	100.5

A scheme of the geometric structures of the $[Pt(CNMe)_2(CN)_2]_n$ (n = 2–4) species in the S_0 and T_1 state is presented in Figure 3 to intuitively understand the geometry change upon oligomerization. Three points can be drawn from Figure 3. (1) The chain of the complexes is straighter in the T_1 state than in the S_0 state, as reflected by the smaller α angles and larger Pt–Pt–Pt bond angles. (2) In the dimer, a larger reduction (ca. 13%) of the Pt–Pt distance on going from the S_0 state to the T_1 state is observed, whereas a smaller reduction of 6–8% occurs in the trimer and tetramer. This larger contraction in the dimer implies that the dimer in the triplet excited state may be the most stable species in $[Pt(CNMe)_2(CN)_2]_n$. This conclusion is in agreement with that by Rillima et al.[33] for the platinum(II) diphenyl dicarbonyl complex. (3) With respect to the trimer in both the S_0 and T_1 state, the distance between one pair of adjacent monomers is smaller than that between the other pair. The case is different for the tetramer; the distance between the central two monomers (Pt2–Pt3) is much smaller than that between the other adjacent pairs (Pt1–Pt2 and Pt3–Pt4). In fact, there are two different interactions in the trimer and tetramer, e.g. intramolecular and intermolecular interactions. In **2**–**4**, the Pt1–Pt2 interactions of **2** and **3** and the Pt2–Pt3 interactions of **4** are intramolecular contacts (d1), while the Pt2–Pt3 interactions of **3** and the Pt1–Pt2 and Pt3–Pt4 interactions of **4** are of the intermolecular type (d2). We can see that the d1 distances are moderately shorter than the d2 distances, and d1 gradually decreases on going from the trimer to tetramer. With reference to previous remarks by Novoa et al.,[35] in platinum(II) dimers, four electrons in one Pt–Pt bond contribute to the excess electrons in the z direction. If the trimer or tetramer can be treated as a special dimer in which a monomer is bonded

to the axial positions, the attacked Pt^{II} unit could act as a base and could contribute two d_{z^2} electrons to bind in the axial direction in a face-to-face fashion. Therefore, the forming of two or three bonds with a total of six or eight d_{z^2} electrons will result in a greater excess of *z* electron density and enhance the interactions of the stacked complexes. Preliminary extended Hückel calculations[36] on the corresponding d^8–d^8 dimers suggested that binding of Lewis acid and/or base to metal atoms at the axial positions has an increasing effect on the M–M bond strength. Our results are in agreement with these conclusions, and excess electrons in the axial direction can account for the variation in the Pt–Pt distance.

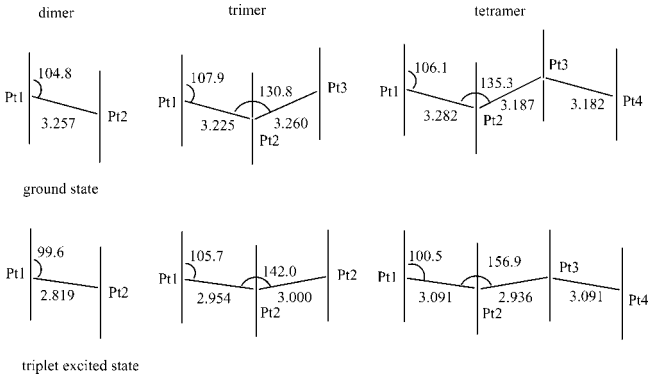

Figure 3. Schematic representation of the S_0 and T_1 structures for **2**–**4**.

The above description is based on only a qualitative analysis, quantitative proof must be obtained with the bond order indices. Bond order is a measure of the number of bonding electron pairs between atoms. Here, we use bond order to qualitatively compare the relative strength of the Pt–Pt bond in **2**–**4**. As suggested previously in the literature,[12a,12b] the Pt–Pt bonding of such complexes is mainly determined by the electrons in the $\sigma[d_{z^2}(Pt_2)]$ and $\sigma^*[d_{z^2}(Pt_2)]$ orbitals. We investigated the Pt–Pt bonding for **2**–**4** by using the Wiberg bond indices (WBIs)[37] in the Natural Bond Orbital (NBO 5.0) program;[38] the details of the WBIs are presented in Table 5. As seen from Table 5, the Pt–Pt WBIs in **2**–**4** are 0.0141 (**2**), 0.0157 and 0.0149 (**3**), and 0.0139, 0.0199, and 0.0139 (**4**), respectively, and they are one magnitude order less than that of an ordinary single bond (for example: Pt1–C3 WBI in **2** is 0.5445), which implies that the Pt–Pt bond is weak. There is a correlation between Pt–Pt WBIs and Pt–Pt bond lengths – the shorter the bond length, the higher the WBI. Therefore, the largest WBI (Pt2–Pt3, 0.0199 in **4**) results in the shortest Pt–Pt contact in **2**–**4**. From another point of view, the proportion of $\sigma[d_{z^2}(Pt_2)]$ orbitals relative to $\sigma^*[d_{z^2}(Pt_2)]$ orbitals in Pt2–Pt3 of **4** is the largest.

We have analyzed the effect of aggregation on the Pt–Pt distances, we will now further discuss the effect on the HOMO–LUMO gap for the $[Pt(CNMe)_2(CN)_2]_n$ (n = 1–4) species. Figure 4 shows the trend in the HOMO–LUMO gap as the value of n increases. A progressive reduction in the HOMO–LUMO gap is observed upon aggregation. The

Table 5. Wiberg bond orders of **2**–**4** calculated by the program NBO 5.0.

		Pt1–Pt2	Pt2–Pt3	Pt3–Pt4
2	Bond length [Å]	3.257	–	–
	WBI	0.0141	–	–
3	Bond length [Å]	3.225	3.260	–
	WBI	0.0157	0.0149	–
4	Bond length [Å]	3.282	3.187	3.182
	WBI	0.0139	0.0199	0.0139

HOMOs for **2**–**4** are all of the $d_{\sigma^*}(d_{z^2}$–$d_{z^2})$ type, while the LUMOs are mainly localized on the mixed $p_\sigma(p_z$–$p_z)$ and *iso*-CN^- π orbital. The reduction in the HOMO–LUMO gap due to 1D aggregation is a result of concomitant destabilization of the HOMOs and stabilization of the LUMOs. It is noticeable that the decrease in the energy of the LUMOs is more gentle than the increase in energy of the HOMOs, which implies that aggregation has a greater impact on $d_{\sigma^*}(d_{z^2}$–$d_{z^2})$ than on $p_\sigma(p_z$–$p_z)$. This observation is in agreement with the results predicted by other calculations. We do not consider 2D aggregation similar to that observed in $[Au(CN)^-]_n$, because 2D aggregation is prohibited from the square-planar geometry of the Pt^{II} atom.

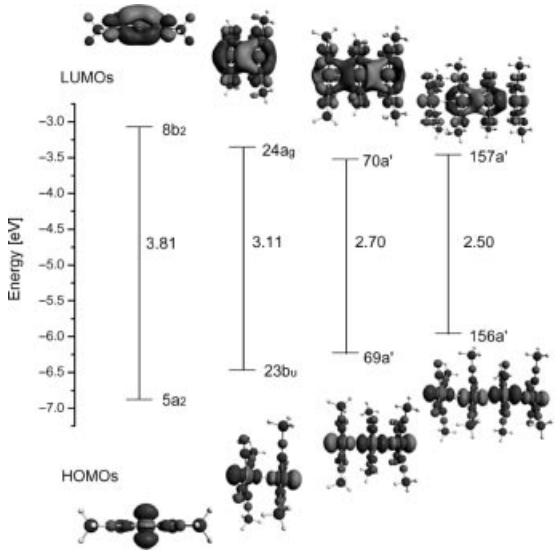

Figure 4. The HOMO and LUMO energy levels for **1**–**4** in the S_0 state.

On the basis of the optimized T_1 geometry for the $[Pt(CNMe)_2(CN)_2]_n$ (n = 1–4) species, the emission spectra were determined by the TD-DFT method embedded in the ADF2005.01 package (see Table 6). As shown in Figure 4, the emissions are all attributed to the excitation of HOMO→LUMO, and the emission energies decrease in the order **1** > **2** > **3** > **4**, in accordance with the sequence of the HOMO–LUMO gap. The emission energies of **1** and **2** calculated by VWN DF are close to those calculated by the MP2 method, which shows the relative reliability of the DFT approach. With respect to the four lowest-energy excite states, $^3B_2$, ^3B_u, $^3A'$, and $^3A'$, the excitation configura-

tion of HOMO→LUMO contributes the largest weight of ca. 0.99 and should be responsible for the character of the emissions. According to above description, the emissions of **1** and **2** are identical to those predicted by the MP2 method and arise from the d_{z^2}→p_z/*iso*-CN^- transitions (MC and MLCT) for **1** and d_{σ^*}→p_σ/*iso*-CN^- transitions (MC and MLCT) for **2**. It should be noted that the emission energies for **3** and **4** are red-shifted by ca. 0.21 and 0.53 eV relative to **2**, respectively. Although the Pt–Pt intramolecular distances for **3** and **4** are shorter than that for **2**, the contraction of intramolecular contacts alone cannot account for the distinctive red-shift. For example, our previous work showed that the Pt–Pt distance in $[Pt_2(pop)_4]^{4-}$ is ca. 0.08 Å shorter than that in $[Pt_2(pcp)_4]^{4-}$ (pop = $P_2O_5H_2^{2-}$ and pcp = $P_2O_4CH_4^{2-}$), but the difference in their emission energies is only 0.07 eV. Thus, we conceive that the intermolecular $5d_{z^2}$–$5d_{z^2}$ interactions also play an important role in the red-shift of the emission energy. The 557 and 650 nm emissions for **3** and **4** are attributed to the combination of intermolecular and intramolecular d_{σ^*}→p_σ/*iso*-CN^- transitions (intra/inter MC and MLCT). This can be intuitively understood from the electron density diagram (Figure 4). This assignment also indicates that the 584 nm emission observed experimentally may arise from the combined contribution of the trimer and tetramer oligomers.

Table 6. Emissions of **1**–**4** in CH_3CN solution determined by TD-DFT (VWN/BP86) calculations.

	Excited state	Configuration (contribution weight)	*E* [eV] (λ [nm]) Calcd.	Exp.
monomer	$^3B_2$	$16a_2$→$8b_2$ (0.99)	3.81 (326)	–
dimer	^3B_u	$23b_u$→$24a_g$(0.99)	2.44 (509)	2.34 (530)[a]
trimer	$^3A'$	69a′→70a′(0.99)	2.23 (557)	2.13 (584)[a]
tetramer	$^3A'$	156a′→157a′(0.99)	1.91 (650)	2.13 (584)[a]

[a] Ref.[13]

Conclusions

We explored the electronic properties of the S_0 and T_1 states of $[Pt(CNMe)_2(CN)_2]_n$ (n = 1–2) complexes at the MP2 and UMP2 levels. The geometrical parameters of the monomer and dimer are in agreement with that observed experimentally. In the S_0 state, the calculated Pt–Pt distance of the dimer is 3.154 Å. The shorter Pt–Pt distance than the van der Waals distance of 3.2 Å indicates the presence of a weak interaction between the two platinum(II) atoms, and the frequency calculations further prove that there is a weak bonding interaction. In the T_1 state, the Pt–Pt distance undergoes a significant reduction, which results from the promotion of an electron from the σ*[$Pt(d_{z^2})$] to σ[$Pt(p_z)$] orbital. As a consequence, a red-shift in the emission energy is observed from monomer to dimer, and the luminescence arises from the $^3[d_{\sigma^*}p_\sigma]$ excited state.

The slate type VWN functional in the DF method was used to predict the impact of oligomerization on $[Pt(CNMe)_2(CN)_2]_n$ (n = 1–4). In the calculation, the dimer is proposed to be the most stable form in the solid state and in solution. The trimer and tetramer can be treated as a special dimer in which the donor ligand is bonded to the central Pt atoms of the dimer. The excess z electrons increase the electron density localized on the Pt–Pt bond and hence enhance the strength of the Pt–Pt bonding. The Pt–Pt distance in the tetramer (3.187 Å) is the shortest, which is consistent with the highest WBI in the investigated Pt–Pt bond.

The experimentally observed lower- and higher-energy emission bands result from the different oligomers in solution. The emission at 530 nm mainly originates from the dimer, while the lower-energy emission at 584 nm derives from the associated contribution of the trimer and tetramer. It should be noted that, aside from intramolecular Pt–Pt interactions, intermolecular Pt–Pt contacts also plays an important role in the red-shift of the emission energy.

Acknowledgments

This work is supported by the Natural Science Foundation of China (20173021, 20333050, 20573042), Natural Science Foundation of Heilongjiang Province of China (No. B200601), and Science Foundation for Excellent Youth of Heilongjiang University of China (No. JC2006L2).

[1] a) H. Yersin, *J. Chem. Phys.* **1978**, *68*, 4707–4713; b) W. A. Fordyce, J. G. Brummer, G. A. Crosby, *J. Am. Chem. Soc.* **1981**, *103*, 7061–7064; c) C. Bellitto, A. Flamini, O. Piovesana, P. F. Zanazzi, *Inorg. Chem.* **1980**, *19*, 3632–3636; d) P. Stein, M. K. Dickson, D. M. Roundhill, *J. Am. Chem. Soc.* **1983**, *105*, 3489–3494; e) V. M. Miskowski, V. H. Houlding, *Inorg. Chem.* **1991**, *30*, 4446–4452.

[2] a) A. P. Zipp, *Coord. Chem. Rev.* **1988**, *84*, 47–83; b) D. M. Roundhill, H. B. Gray, C. M. Che, *Acc. Chem. Res.* **1989**, *22*, 55–61; c) B.-H. Xia, C.-M. Che, D. L. Phillips, K.-H. Leung, *Inorg. Chem.* **2002**, *41*, 3866–3875; d) C.-M. Che, V.-W.-W. Yam, W.-T. Wong, T.-F. Lai, *Inorg. Chem.* **1989**, *28*, 2908–2910; e) B.-H. Xia, C.-M. Che, Z.-Y. Zhou, *Chem. Eur. J.* **2003**, *9*, 3055–3064; f) H.-K. Yip, T.-F. Lai, C.-M. Che, *J. Chem. Soc., Dalton Trans.* **1991**, 1639–1641.

[3] a) R. Büchner, C. T. Cunningham, J. S. Field, R. J. Haines, D. R. McMillin, G. Summerton, *J. Chem. Soc., Dalton Trans.* **1999**, 711–718; b) W. B. Connick, R. E. Marsh, W. P. Schaefer, H. B. Gray, *Inorg. Chem.* **1997**, *36*, 913–922; c) E. M. Ratilla, B. K. Scott, M. S. Moxness, N. M. Kostic, *Inorg. Chem.* **1990**, *29*, 918–926; d) Y. Chen, J. W. Merkert, Z. Murtaza, C. Woods, D. P. Rillema, *Inorg. Chim. Acta* **1995**, *240*, 41–47.

[4] W. A. Fordyce, J. G. Brummer, G. A. Grosby, *J. Am. Chem. Soc.* **1981**, *103*, 7061–7064.

[5] a) C.-M. Che, L. G. Butler, H. B. Gray, *J. Am. Chem. Soc.* **1981**, *103*, 7796–7797; b) S. F. Rice, H. B. Gray, *J. Am. Chem. Soc.* **1983**, *105*, 4571–4575.

[6] a) W. B. Heuer, M. D. Totten, G. S. Rodman, E. J. Hebert, H. J. Tracy, J. K. Nagle, *J. Am. Chem. Soc.* **1984**, *106*, 1163–1164; b) J. R. Peterson, K. Kalyanasundaram, *J. Phys. Chem.* **1985**, *89*, 2486–2492; c) M. S. Herman, J. L. Goodman, *Inorg. Chem.* **1991**, *30*, 1147–1149.

[7] a) D. M. Roundhill, *J. Am. Chem. Soc.* **1985**, *107*, 4354–4356; b) D. M. Roundhill, S. J. Atherton, *Inorg. Chem.* **1986**, *25*, 4071–4072; c) D. M. Roundhill, Z. P. Shen, S. J. Atherton, *Inorg. Chem.* **1987**, *26*, 3833–3835.

[8] a) A. Vlcek Jr, H. B. Gray, *Inorg. Chem.* **1987**, *26*, 1997–2001; b) E. L. Harvey, A. E. Stiegman, A. Vlcek Jr, H. B. Gray, *J. Am. Chem. Soc.* **1987**, *109*, 5233–5235; c) C.-M. Che, W.-M.

Lee, K.-C. Cho, P. D. Harvey, H. B. Gray, *J. Phys. Chem.* **1989**, *93*, 3095–3099; d) R. J. Sweeney, E. L. Harvey, H. B. Gray, *Coord. Chem. Rev.* **1990**, *105*, 23–24.

[9] a) W. A. Kalsbeck, N. Grover, H. H. Thorp, *Angew. Chem. Int. Ed. Engl.* **1991**, *30*, 1517–1518; b) W. A. Kalsbeck, D. M. Gingell, J. E. Malinsky, H. H. Thorp, *Inorg. Chem.* **1994**, *33*, 3313–3316; c) S. A. Ciftan, H. H. Thorp, *J. Am. Chem. Soc.* **1998**, *120*, 9995–10000.

[10] M. K. Dickson, S. K. Pettee, D. M. Roundhill, *Anal. Chem.* **1981**, *53*, 2159–2160.

[11] D. M. Roundhill, *Sol. Energy* **1986**, *36*, 297–299.

[12] a) I. V. Novozhilova, A. V. Volkov, P. Coppens, *J. Am. Chem. Soc.* **2003**, *125*, 1079–1087; b) S. R. Stoyanov, J. M. Villegas, D. P. Rillema, *J. Phys. Chem. B* **2004**, *108*, 12175–12180.

[13] Y.-H. Sun, K.-Q. Ye, H.-Y. Zhang, J.-H. Zhang, L. Zhao, B. Li, G. D. Yang, B. Yang, Y. Wang, S.-W. Lai, C.-M. Che, *Angew. Chem. Int. Ed.* **2006**, *45*, 5610–5613.

[14] a) C. E. Buss, C. E. Anderson, M. K. Pomije, C. M. Lutz, D. Britton, K. R. Mann, *J. Am. Chem. Soc.* **1998**, *120*, 7783–7790; b) C. E. Buss, K. R. Mann, *J. Am. Chem. Soc.* **2002**, *124*, 1031–1039; c) C. L. Exstrom, J. R. Sowa Jr, C. A. Daws, D. Janzen, K. R. Mann, *Chem. Mater.* **1995**, *7*, 15–17; d) C. A. Daws, C. L. Exstrom, J. R. Sowa Jr, K. R. Mann, *Chem. Mater.* **1997**, *9*, 363–368; e) C. L. Exstrom, M. K. Pomije, K. R. Mann, *Chem. Mater.* **1998**, *10*, 942–945.

[15] a) H.-X. Zhang, C.-M. Che, *Chem. Eur. J.* **2001**, *7*, 4887–4893; b) Q.-J. Pan, H.-X. Zhang, *Organometallics* **2004**, *23*, 5198–5209; c) Q.-J. Pan, H.-G. Fu, H.-T. Yu, H.-X. Zhang, *Inorg. Chem.* **2006**, *45*, 8729–8735.

[16] M. J. Frisch, G. W. Trucks, H. B. Schlegel, G. E. Scuseria, M. A. Robb, J. R. Cheeseman, J. A. Montgomery Jr, T. Vreven, K. N. Kudin, J. C. Burant, J. M. Millam, S. S. Iyengar, J. Tomasi, V. Barone, B. Mennucci, M. Cossi, G. Scalmani, N. Rega, G. A. Petersson, H. Nakatsuji, M. Hada, M. Ehara, K. Toyota, R. Fukuda, J. Hasegawa, M. Ishida, T. Nakajima, Y. Honda, O. Kitao, H. Nakai, M. Klene, X. Li, J. E. Knox, H. P. Hratchian, J. B. Cross, C. Adamo, J. Jaramillo, R. Gomperts, R. E. Stratmann, O. Yazyev, A. J. Austin, R. Cammi, C. Pomelli, J. W. Ochterski, P. Y. Ayala, K. Morokuma, G. A. Voth, P. Salvador, J. J. Dannenberg, V. G. Zakrzewski, S. Dapprich, A. D. Daniels, M. C. Strain, O. Farkas, D. K. Malick, A. D. Rabuck, K. Raghavachari, J. B. Foresman, J. V. Ortiz, Q. Cui, A. G. Baboul, S. Clifford, J. Cioslowski, B. B. Stefanov, G. Liu, A. Liashenko, P. Piskorz, I. Komaromi, R. L. Martin, D. J. Fox, T. Keith, M. A. Al-Laham, C. Y. Peng, A. Nanayakkara, M. Challacombe, P. M. W. Gill, B. Johnson, W. Chen, M. W. Wong, C. Gonzalez, and J. A. Pople, *Gaussian 03, Revision B.03*, Gaussian, Inc. Pittsburgh PA, **2003**.

[17] C. Møller, M. S. Plesset, *Phys. Rev.* **1934**, *46*, 618–622.

[18] a) M. E. Casida, C. Jamorski, K. C. Casida, D. R. Salahub, *J. Chem. Phys.* **1998**, *108*, 4439–4449; b) C. Jamorski, M. E. Casida, D. R. Salahub, *J. Chem. Phys.* **1996**, *104*, 5134–5147; c) R. E. Statmann, G. E. Scuseria, *J. Chem. Phys.* **1998**, *109*, 8218–8224; d) R. Bauernschmitt, R. Ahlrichs, *Chem. Phys. Lett.* **1996**, *256*, 454–464; e) N. Matsuzawa, N. A. Ishitani, D. Dixon, A. T. Uda, *J. Phys. Chem. A* **2001**, *105*, 4953–4962.

[19] J. P. Perdew, K. Burke, M. Ernzerhof, *Phys. Rev. Lett.* **1996**, *77*, 3865–3868.

[20] a) S. Miertuš, E. Scrocco, J. Tomasi, *Chem. Phys.* **1981**, *55*, 117; b) E. Cancès, B. Mennucci, J. Tomasi, *J. Chem. Phys.* **1997**, *107*, 3032–3041; c) V. Barone, M. Cossi, J. Tomasi, *J. Comput. Chem.* **1998**, *19*, 404–417.

[21] a) W. R. Wadt, P. J. Hay, *J. Chem. Phys.* **1985**, *82*, 284–298; b) P. J. Hay, W. R. Wadt, *J. Chem. Phys.* **1985**, *82*, 299–310.

[22] P. Pyykkö, F. Mendizabal, *Inorg. Chem.* **1998**, *37*, 3018–3025.

[23] a) G. Te Velde, F. M. Bickelhaupt, S. J. A. van Gisbergen, C. Fonseca Guerra, E. J. Baerends, J. G. Snijders, T. Ziegler, *J. Comput. Chem.* **2001**, *22*, 931–967; b) C. Fonseca Guerra, J. G. Snijders, G. Te Velde, E. J. Baerends, *Theor. Chem. Acc.* **1998**, *99*, 391–403; c) *Vrije ADF 2005.01*, SCM, Amsterdam, **2005**.

[24] a) P. Pyykkö, N. Runerberg, *Chem. Phys. Lett.* **1994**, *218*, 133; b) P. Pyykkö, Y. F. Zhao, *Angew. Chem. Int. Ed. Engl.* **1991**, *30*, 604–605; c) P. Pyykkö, N. Runerberg, F. Mendizabal, *Chem. Eur. J.* **1997**, *3*, 1451–1456.

[25] S.-G. Wang, W. H. Eugen Schwarz, *J. Am. Chem. Soc.* **2004**, *126*, 1266–1276.

[26] a) M. A. Rawashdeh-Omary, M. A. Omary, H. H. Patterson, *J. Am. Chem. Soc.* **2000**, *122*, 10371–10380; b) M. A. Rawashdeh-Omary, M. A. Omary, H. H. Patterson, J. P. Fackler Jr, *J. Am. Chem. Soc.* **2001**, *123*, 11237–11247.

[27] S. H. Vosko, L. Wilk, M. Nusair, *Can. J. Phys.* **1980**, *58*, 1200–1210.

[28] a) T. Ziegler, J. G. Snijders, E. J. Baerends, *J. Chem. Phys.* **1981**, *74*, 1271–1281; b) E. van Lenthe, E. J. Baerends, J. G. Snijders, *J. Chem. Phys.* **1994**, *101*, 9783–9792; c) E. van Lenthe, E. J. Baerends, J. G. Snijders, *J. Chem. Phys.* **1993**, *99*, 4597–4610; d) E. van Lenthe, R. van Leeuwen, E. J. Baerends, J. G. Snijders, *Int. J. Quantum Chem.* **1996**, *57*, 281–293; e) E. van Lenthe, A. E. Ehlers, E. J. Baerends, *J. Chem. Phys.* **1999**, *110*, 8943–8953.

[29] F. Eckert, A. Klamt, *AIChE J.* **2002**, *48*, 369–385.

[30] a) A. D. Becke, *Phys. Rev. A* **1988**, *38*, 3098–3100; b) J. P. Perdew, *Phys. Rev. B* **1986**, *33*, 8822–8824.

[31] Q.-J. Pan, H.-X. Zhang, X. Zhou, H.-G. Fu, H.-T. Yu, *J. Phys. Chem. A* **2007**, *111*, 287–294.

[32] W. B. Connick, R. E. Marsh, W. P. Schaefer, H. B. Gray, *Inorg. Chem.* **1997**, *36*, 913–922.

[33] S. R. Stoyanov, J. M. Villegas, D. P. Rillema, *Inorg. Chem.* **2003**, *42*, 7852–7860.

[34] J. W. Schindler, R. C. Fukuda, A. W. Adamson, *J. Am. Chem. Soc.* **1982**, *104*, 3596–3600.

[35] J. J. Novoa, G. A. Pere Alemany, S. Alvarez, *J. Am. Chem. Soc.* **1995**, *117*, 7169–7171.

[36] K. R. Mann, J. G. Gordon, H. B. Gray, *J. Am. Chem. Soc.* **1975**, *97*, 3553–3555.

[37] C. M. Breneman, K. B. Wiberg, *J. Comput. Chem.* **1990**, *11*, 361–373.

[38] E. D. Glendening, . J. K. Badenhoop, A. E. Reed, J. E. Carpenter, J. A. Bohmann, C. M. Morales, F. Weinhold, *NBO 5.0*, Theoretical Chemistry Institute, University of Wisconsin, Madison, WI, **2001**.

Received: January 8, 2007
Published Online: April 10, 2007

